Middle-Ear Stiffness of the Bottlenose Dolphin
Tursiops truncatus

Brian S. Miller, Aleks L. Zosuls, Darlene R. Ketten, and David C. Mountain

Abstract—Previous research on the cetacean auditory system has consisted mostly of behavioral studies on a limited number of species. Little quantitative physiologic data exists on cetacean hearing. The frequency range of hearing varies greatly across different mammalian species. Differences among species correlate with differences in the middle-ear transfer function. Middle-ear transfer functions depend on the mechanical stiffness of the middle ear and the cochlear input impedance. The purpose of this study was to measure the middle-ear stiffness for the bottlenose dolphin (*Tursiops truncatus*), a species specialized for underwater high-frequency hearing and echolocation. Middle-ear stiffness was measured with a force probe that applied a known displacement to the stapes and measured the restoring force. The average middle-ear stiffness in ten dolphin ears was 1.37 N/μm, which is considerably higher than that reported for most terrestrial mammals. The relationship between middle-ear stiffness and low-frequency hearing cutoff in *Tursiops* was shown to be comparable to that of terrestrial mammals.

Index Terms—Acoustic power flow, cetacea, hearing range, middle ear, odontocete, stiffness.

I. INTRODUCTION

CETACEANS have advanced auditory systems and are capable of hearing underwater at least as well as, if not better than, humans in air. Odontocetes, or toothed whales, produce ultrasonic echolocation signals to forage and hunt, while mysticetes (baleen whales) produce infrasonic sounds containing frequencies as low as 10 Hz [1]. Because hearing is arguably a principal sense for whales and because it takes place underwater, it is reasonable to assume that the cetacean auditory system is highly derived. However, few physiological studies have been conducted to determine the nature of these specializations due in part to the difficulties and expense of keeping live captive marine mammals as well as the legal restrictions on research activities related to their protected status. Understanding the cetacean auditory system could provide insights into hearing in general, and may be useful for comparative studies of hearing in other species.

In addition to studying cetacean hearing for the purposes of comparative anatomy and physiology, there is a need to understand cetacean hearing for the purposes of conservation. Cetaceans may be in danger from man-made noise in the
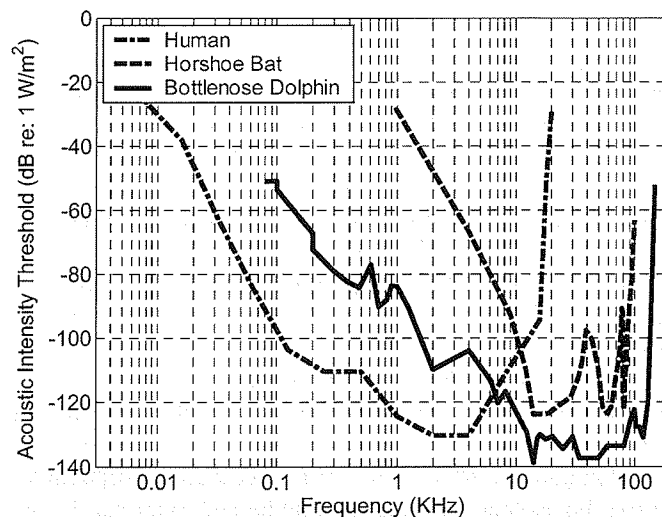
Fig. 1. Audiograms of the fruit bat *Rhinolophus ferrumquinum* [5], a human [4], and the bottlenose dolphin *Tursiops truncatus* are plotted as against intensity. Intensity rather than sound-pressure level is plotted to allow direct comparison of aquatic and terrestrial species [3].

oceans, which can include noise from commercial, industrial, scientific, and military activities. Because hearing is a crucial sense for cetaceans, noise can harm these animals either directly through physical damage to their auditory system or indirectly through impacts on behavior.

Most research on odontocete hearing consists of behavioral tests [2]. These psychophysical experiments are expensive and require great efforts to maintain and train the animals tested, but they can determine some hearing characteristics, such as the range, critical ratios, and thresholds for each animal tested. A classic example of such psychophysical experiments is the generation of the behavioral audiogram. An audiogram is a measure of a subject's hearing threshold, defined to be the smallest audible sound intensity at a given frequency, plotted as a function of frequency. Fig. 1 shows the audiogram of the bottlenose dolphin *Tursiops truncatus* [3] compared to a human [4] and a horseshoe bat [5].

The audiogram can be thought of as an inverse transfer function of the hearing system where threshold is measured in place of gain. As one can see from Fig. 1, there is considerable diversity both in the high- and low-frequency limits of the audiogram.

The "black-box" approach of these behavioral experiments, however, reveals little information about the mechanics of the auditory system. Furthermore, the characteristics measured vary from species to species, and captive testing of most whales and dolphins, which are large and endangered, is not practical. Understanding the mechanics of the system could allow for a more

generalized model of cetacean hearing, which could be applied to species that are not feasible for conventional audiometric testing.

A. Auditory Anatomy

The peripheral auditory system of terrestrial mammals can be divided into three main areas: The outer ear, middle ear, and inner ear. The outer ear, which consists of the pinna and auditory canal, functions to deliver sound from the environment to the middle ear for further processing. This portion of the system functions as a filter with a complex frequency response that depends on sound-source location (head-related transfer function). The middle ear, which consists of the eardrum and ossicles, functions to match the impedance of the airborne sound to the impedance of the fluid-filled cochlea. The inner ear or cochlea functions as a mechanical filter bank with each filter tuned to a different frequency. The outputs of these filters are encoded into electrical signals that are passed on to the brain via the auditory nerve [6].

The first stage in the peripheral auditory system of odontocetes appears to differ in several ways from that of terrestrial mammals. Odontocetes have no external pinna, and, unlike terrestrial mammals, the auditory canal is occluded. Furthermore, the two bones that surround the middle and inner ear, known as the tympano–periotic complex, comprise bullae that are suspended in a cavity outside the skull. The tympanic membrane or eardrum is vastly different in form and possibly in function from its terrestrial counterpart while the odontocete cochlea appears to have the same basic organization as other mammalian inner ears [1].

1) Outer Ear: Since odontocetes do not have a traditional outer ear, references to the odontocete "outer ear" should be taken to mean the soft-tissue sound pathways to the tympano–periotic bullae. While the exact means of sound conduction from the exterior to the middle ear is not known, it may be possible to discover this pathway by working backward from within the cochlea outward through the middle ear to identify the tissue and points of middle-ear inputs and what constitutes the tympanic-membrane analog.

2) Middle Ear: The middle ear is bounded by the tympanic and periotic bones (Fig. 2). This tympano–periotic complex houses the three bones that comprise the ossicular chain. Unlike other mammals, the odontocete bulla is not fused to the skull; rather, it is a free-standing structure surrounded on all sides by soft tissues. The auditory ossicles, malleus (M), incus (I), and stapes (S), are shown in Fig. 2. The malleus is fused to the tympanic bone along the extended tapered malleal arm. The malleo–incudal joint between the malleus and incus is typically saddle shaped and reinforced by stiff ligaments. The footplate of the stapes lies in the oval window of the periotic bone, which marks the entrance to the cochlea and the inner ear. The stapes footplate is secured in the oval window by a relatively stiff annular ligament, which in some individual animals is partially calcified [1], [7], [8].

3) Inner Ear: The inner ear consists of the fluid-filled spiral cochlea, which is divided into three compartments or scalae by two membranes: Reissner's membrane (between scala vestibulae and scala media) and the basilar membrane
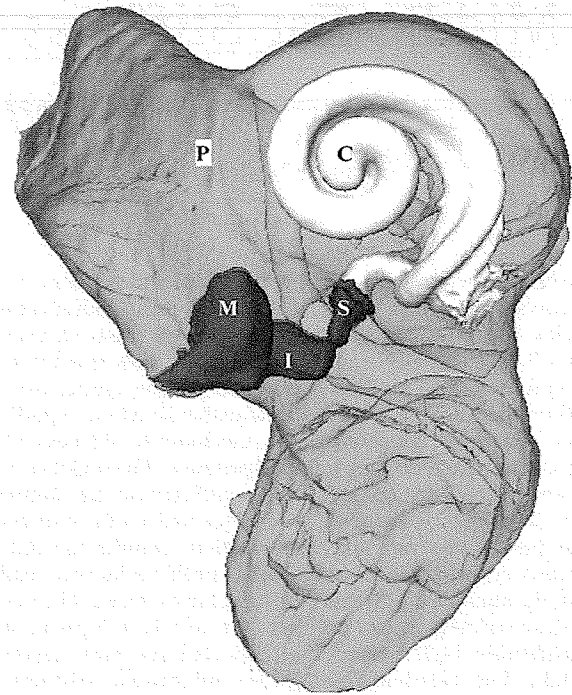

Fig. 2. Cut away view of periotic bone (P), malleus (M), incus (I), stapes (S), and cochlear duct (C). The malleus attaches to the tympanic bone (not shown) and the incus in a very firm connection. The incus and stapes are connected by ligaments. The oval window is a window in the periotic bone at the junction of the stapes and cochlear duct. The cochlear duct shown above includes all scalae and is overlaid on the periotic bone for clarity.

(between scala media and scala tympani). Fig. 2(c) shows all three compartments of the cochlea as a single structure. The sensory receptor cells (hair cells) are arrayed along the basilar membrane and convert mechanical acoustic inputs into electrical potentials. These signals are transmitted to the spiral ganglion cells, and thus to the brain, via the auditory nerve fibers.

The middle-ear ossicles drive the cochlea via a pistonlike movement of the stapes footplate in the oval window, causing a pressure difference between the oval and round windows [1], [8], [9]. It is believed that the odontocete cochleae function in the same manner as those of terrestrial mammals [1], [8]–[11], i.e., the pressure difference between the oval and round windows allows a traveling wave within the cochlea to displace the basilar membrane. Peaks in the traveling wave vary longitudinally along the basilar membrane as a function of membrane resonance response characteristics versus signal frequencies. The basal end of the cochlea is stimulated best by high frequencies, while low-frequency responses are greatest at the apex. For most of the cochlea, membrane deformations are characterized by a shallow low-frequency slope and steep high-frequency slope. The steep high-frequency slope in the basilar membrane response at the extreme basal end of the cochlea is believed to be responsible for the steep slope of the high-frequency portion of the audiogram [12].

B. Acoustic-Power-Flow Model

A common approach in modeling the auditory periphery is to start with an acoustic-power-flow model in which the external ear, middle ear, and cochlea are treated as a series of connected
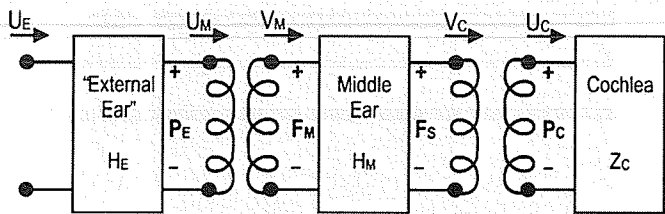
Fig. 3. Schematic diagram of the acoustic-power-flow model of hearing. External, middle, and inner ear (cochlea) are each represented as two-port networks connected by transformers. Transformers are used to represent the conversion of pressures to forces and volume velocities to particle velocities, which occurs between the external, middle, and inner ear. The external ear and cochlea are written using an acoustic-impedance analogy, while the middle ear is written using a mechanical-impedance analogy.
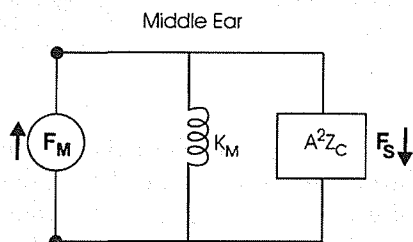

Fig. 4. Simplified model of the middle ear and cochlea derived from the acoustic-power-flow model. Note that this model makes use of the electomechanical mobility analogy. The middle ear is represented as a spring with stiffness K_M. F_M is the force through the middle ear. The cochlea is represented as an impedance Z_C multiplied by the transformer ratio A_S^2, which is the area of the stapes footplate squared.

acoustical and mechanical systems where outputs from each system provide the inputs for the next [6]. The mechano-acoustical system comprised of the outer and middle ear (Fig. 3) is modeled as a transformer-coupled pair of two-port networks. The two-port blocks represent the acoustic and mechanical transfer functions of the external ear (H_E) and the middle ear (H_M) respectively. The cochlear block represents the acoustic input impedance Z_C of the cochlea. The transformer between the external ear and middle ear converts acoustic volume velocity and acoustic pressure U_M and P_M to mechanical velocity V_M and force F_M, respectively, while the transformer between the middle ear and cochlea converts the mechanical velocity and force V_C and F_C of the ossicular chain back into acoustic velocity and pressure, U_C and P_C, respectively.

Measurements have been made of the middle-ear input impedance $Z_M = F_M/V_M$ in terrestrial mammals. These show that Z_M is stiffness dominated at low frequencies and becomes resistive at higher frequencies due to cochlear loads.

It is believed that both inner and middle-ear characteristics determine the shape of the mammalian audiogram, but the low- and mid-frequency portions of the audiogram are influenced most by the middle-ear transfer function [13]. For an in-depth review of the acoustic-power-flow model, see [6].

Fig. 4 shows a simplified mechanical model of the middle and inner ear derived from the acoustic-power-flow model (Fig. 3). In this model, the middle-ear block is approximated by an ideal spring (K_M). The acoustic impedance of the cochlea has been converted to a mechanical impedance by multiplying it by the

transformer ratio A_S^2, where A_S is the area of the stapes footplate. If we further assume the cochlear input impedance is resistive ($Z_C = R_C$), then the middle-ear transfer function can be expressed as

$$H(f) = \frac{F_s}{F_m} = \frac{jf}{jf + f_c} \qquad (1)$$

where f is the stimulus frequency, and the cutoff frequency f_C (half-power point) is given by

$$f_C = \frac{K_M}{2\pi A_S^2 R_C}. \qquad (2)$$

If this simplified model is correct, then (1) and (2) predict that the middle-ear transfer function can be treated as a high-pass filter with a cutoff frequency proportional to the ratio of the middle-ear stiffness to the cochlear input resistance.

Measurements of A_S are available for many cetacean species [1], [14], [15]; however, there have been no prior quantitative measurements of cochlear input impedance for odontocetes. In one study of the *Tursiops truncatus* middle ear by Fleischer [8], the middle-ear resonant frequency was measured, and stapes mass was used to predict the middle-ear stiffness. He estimated middle-ear stiffness to be 0.6 N/μm, which is consistent with that of echolocating bats. High-frequency species such as bats and dolphins often have bony linkages to the ossicles that increase overall middle-ear stiffness, and the available data suggest that a stiff middle ear is associated with high-frequency hearing [1], [6].

The present study focused on the direct measurement of K_M in the bottlenose dolphin (*Tursiops truncatus*), and on how this value compares with similar measures of stiffness for terrestrial species, to test the hypothesis that middle-ear stiffness correlates with the middle-ear low-frequency cutoff. *Tursiops* was chosen because a wealth of anatomical and behavioral data is available for this species and adequate numbers of ears from stranded animals were available for testing.

II. MATERIALS AND METHODS

A. Ear Preparation

All measurements reported here were made using excised tympano–periotic bones of *Tursiops truncatus*. Samples were obtained postmortem from stranded animals in accordance with normal stranding response procedures and under letters of agreement and research permits issued to Harvard University, Woods Hole Oceanographic Institution, and D.R. Ketten. No animals were euthanized for this study. Because age and life history are generally unknown for most stranded animals and because collection is, of necessity, opportunistic, it was not possible to control absolutely for age, gender, or comparative health of all ears. However, in all cases, the ears were preliminarily screened both grossly and by computerized tomography (CT scanning) to verify that no gross pathology was present. For this preliminary study, to get an adequate sample size, it was necessary to use existing collection material. Therefore, it was not generally possible to extract and measure fresh material. One ear was measured approximately five days after
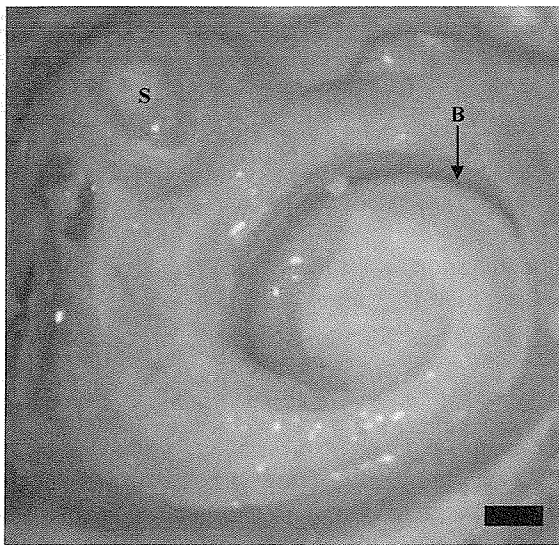
Fig. 5.   Prepared cochlea in the right bulla of a *Tursiops truncatus*. Slightly more than a full turn of the cochlea is exposed. From the basal end at the left, the cochlea spirals counterclockwise and inwards toward the apical end. The basilar membrane (B) can be seen as a black strip in the cochlea. The oval window and stapes footplate (S) can be seen in the upper left-hand corner. The longest dimension of the scale bar in the bottom right corner is 1 mm.
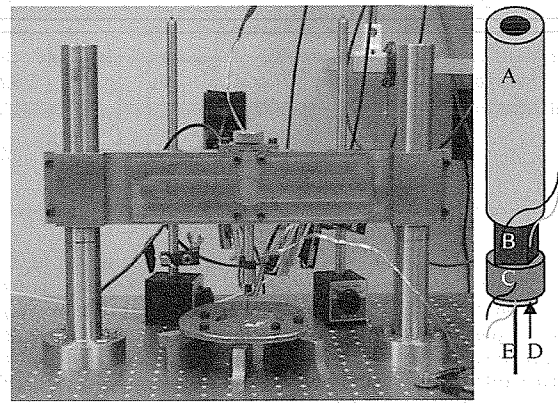

Fig. 6.   Middle-ear measurement apparatus. The ear bones and piezoelectric force probe are attached to a very rigid steel fixture designed to accommodate driving the extremely stiff cetacean ossicular chain. (A) Steel beam. (B) Actuator, a piezoelectric stack. (C) Copper disk. (D) Sensor, a piezoelectric bimorph disk. (E) Steel needle tip.

the death of a euthanized stranded animal that was simply refrigerated. Five left ears obtained from five individuals that died in stranding were frozen immediately postmortem. Four other ears were formalin fixed immediately after death, two right and two left, each from different animals. Testing procedures were the same for all ears, whether refrigerated, frozen, or formalin fixed.

Although most studies of middle-ear stiffness in terrestrial mammals measure middle-ear impedance at the tympanic membrane, anatomical differences between the odontocete tympanic membrane and that of terrestrial animals made this method of measurement questionable for odontocete middle-ear impedance. The model (Fig. 4) suggests that if we remove the cochlear load, K_M can be measured from the internal intracochlear side of the stapes. Therefore, stiffness measurements reported in this paper were made from the cochlear side of the middle ear.

The middle-ear stiffness of these ten ears was measured from within the cochlea using a piezoelectric force probe. To prepare the ear for stiffness measurements, the extracted ears were cleaned of adherent soft tissues. A dental burr was used to expose scala tympani. Additional bone was removed toward the basal end of the cochlea until the vestibule, round window, and stapes footplate were also visible (Fig. 5). The ear was then attached with dental cement to a clamp mounted beneath the force probe (Fig. 6) with the probe needle perpendicular to the stapes footplate. All other ear tissues were left intact and the ears were moistened with a physiological saline solution for the duration of the experiment.

B. Middle-Ear Stiffness Probe

The operating principle of the stiffness probe is the same as that of Olson and Mountain [16], i.e., the probe consists of an active displacement driver in series with a passive piezoelectric

force transducer. Because in these experiments the middle-ear stiffness was anticipated to be at least 0.6 N/μm [8], which is six-orders-of-magnitude larger than the measurements of the basilar membrane stiffness made by Olson and Mountain, special effort was made to stiffen the measurement apparatus.

The middle-ear stiffness probe used a piezoelectric stack to generate displacement and was attached to a piezoelectric disk to sense force. The stack was bonded to a steel post with a precision fit to a heavy steel fixture (Fig. 6). The fixture was fabricated to hold the probe and position it on the stapes footplate. The heavy fixture and a vibration isolation table were required to minimize noise and probe inaccuracies resulting from fixture deflection during measurements. A pin with a tip diameter of approximately 0.5 mm was bonded to the center of the sensing disk for coupling to the stapes footplate. Care was required during positioning to prevent the stapes, annular ligament, or piezo disk from breaking.

1) Middle-Ear Sensor Calibration: The sensor was calibrated by measuring the disk output voltage as the needle tip was driven against steel reference beams of known stiffness. Reference beams had stiffness gradients along their lengths ranging from 0.02 to 20 N/μm, spanning three orders of magnitude around the estimated middle-ear stiffness. The voltage output of the stiffness sensor was then compared to the actual stiffness of the steel reference beam to derive the sensor stiffness or calibration constant.

The reference beams were clamped to the optical table, and the sensor was advanced until the needle tip came into contact with the measurement site on the steel beam. During this step, the driver was set to displace the sensor tip using a small-amplitude sine wave. The presence of the sine wave facilitated the advancement of the probe by allowing visual feedback of when the sensor was in contact. When the sensor tip was not in contact with the reference beam, the sensor output was negligible, but when the sensor tip came into contact with the beam, the output jumped to nearly 20 times that of the noncontact voltage. To ensure that the sensor was in proper contact, the probe was advanced a very short distance very slowly after initial contact was observed until the sensor output remained constant.

All data reported here were obtained with a displacement amplitude of approximately 0.16 μm peak to peak, which is within the range of sound-induced motion of the stapes reported for terrestrial species. Displacements were created using pure tones ranging 50–200 Hz. One thousand epochs of each time-domain waveform were averaged for each frequency to improve signal-to-noise ratio. The frequency range of the probe was limited to 200 Hz due to multiple mechanical resonances at higher frequencies. A high sampling rate (200 kHz) was used for driving the stack to avoid exciting these mechanical resonances. The magnitude and phase of each frequency was obtained by taking the fast Fourier transform (FFT) of the averaged time-domain signal.

After all of the measurement sites were probed, a reference data set was taken with the probe not in contact with the stapes. These data served as a null data set that was subtracted from each measurement to compensate for inertial forces produced by the sensor and needle.

To obtain the sensor stiffness and sensitivity from the reference-beam measurements, the system was treated as a displacement source with two springs in series [17].

C. Middle-Ear Stiffness Measurement

In the experimental ears, the probe was advanced toward the stapes footplate until contact was observed. As noted above, to ensure that the sensor was in proper contact with the stapes, the sensor was advanced a short distance very slowly after initial contact until the sensor output remained constant. During measurements, signal averaging was adjusted between 100 and 3600 sinusoidal presentations per frequency to improve the signal-to-noise ratio.

A fiber-optic displacement probe (Angstrom Resolver, Opto-Acoustic Sensors, inc.) was placed on the footplate of the stapes along with the stiffness sensor, and another fiber-optic probe was placed nearby on the periotic bone to measure differential motion between the stapes and periotic bone. In all cases, the displacement of the periotic bone remained below the 10 nm noise floor. The displacement of the stapes was comparable to the driving displacement of the probe for the duration of the testing.

To estimate the variability that results from differences in positioning the ear in the apparatus, the stiffness of the refrigerated ear, two frozen ears, and two fixed ears were measured several times in a continuous 3 h span as each ear was mounted and repositioned under the measurement apparatus.

To quantify the effects of deterioration over time, two frozen samples and two formalin-fixed samples were retested several days after they were initially tested. During the interval, frozen samples were refrozen, while formalin-fixed samples were placed back in formalin solution.

III. RESULTS

Middle-ear stiffness showed little to no variation with frequency over the frequencies 50–200 Hz. All stiffness data shown here are for 97.7 Hz. Across different samples, stiffness
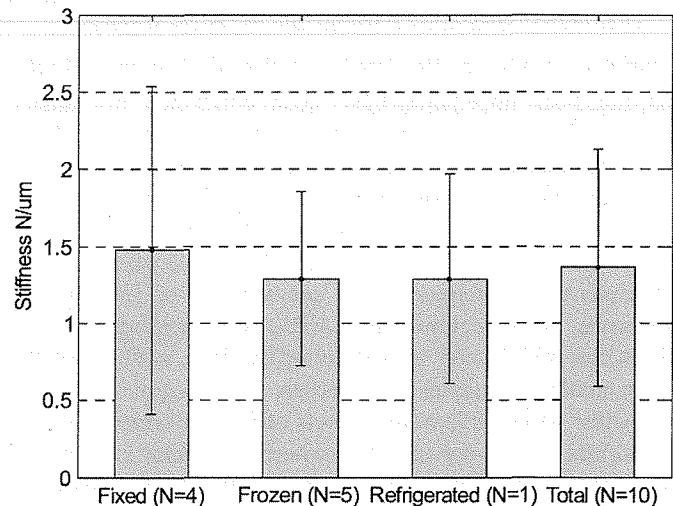

Fig. 7. Mean stiffness for ears grouped by tissue type. There is no significant difference between frozen and formalin-fixed ears. Frozen stiffness = 1.29 ± 0.56 N/μm; fixed stiffness = 1.48±1.06 N/μm; refrigerated stiffness 2.25± 0.78 N/μm; and total stiffness = 1.37±0.77 N/μm. Error bars show standard deviations between different samples, except for the refrigerated ear. The error bar for the refrigerated ear shows the standard deviation of measurements made as the ear was remounted and repositioned seven times in a 3 h time span.

ranged 0.7–3.6 N/μm. The average stiffness for all of the samples was 1.37 N/μm, and the standard deviation across all samples was 0.77 N/μm.

Fig. 7 shows the mean stiffness across samples grouped into frozen ears, fixed ears, and refrigerated ears. T-tests confirmed that there was no significant difference for the mean stiffness of the frozen ears, the fixed ears, and the refrigerated ears ($p > 0.7$). Samples that were remounted and repositioned underneath the apparatus showed a standard deviation of 0.81 N/μm, which is comparable to the standard deviation between samples. Samples showed, on average, a 56% change between the initial testing and retesting up to a week later. However, retesting yielded an increase in stiffness in some samples and a decrease in stiffness for others. The standard deviation between principle and subsequent tests was 0.88 N/μm. A T-test yielded no significant differences between initial and retested measurements despite refreezing of thawed tissues ($p > 0.3$)

IV. DISCUSSION

A. Sources of Variability

Given the large stiffness measured, it can be assumed that the structures contributing the majority of the middle-ear stiffness are of a bony or relatively inelastic nature and will degrade slowly over time. Thus, the ear condition is unlikely to be a major source of error.

Variability measurements suggest that the ear orientation and probe position are responsible for much of the variability observed in the stiffness measurements. It was not possible to consistently mount ears in precisely the same orientation due to variations in shape and size of the ears. This limitation was overcome by mounting and positioning ears several times and averaging the results of these measurements.

B. Anatomical Structures Responsible for High Stiffness

Studies comparing the effects of freezing on the middle- and inner-ear impedance have been conducted in humans [18] and show a two- to threefold decrease in stapes–cochlear input impedance upon freezing the ear. However, in our measurements, no significant difference could be found between frozen tissue, formalin-fixed tissue, and refrigerated tissue. This difference could be due to small sample sizes in both experiments, differences in ear preparation, or fundamental differences in structures responsible for creating stiffness within the middle ear. In particular, the high stiffness of the boney mallear–tymapanic connection in *Tursiops* (a stiffness that is less susceptible to the effects of fixative) may dominate the normal middle-ear stiffness, whereas in other mammalian ears, fixative may greatly affect the controlling stiffnesses of the tympanic membrane and/or ossicular ligaments, leading to significant differences between the stiffness of live and dead ears [7].

Fleischer's prediction of annular-ligament stiffness of 0.6 N/μm in *Tursiops truncatus* is approximately 44% of our mean measured value. Another structure contributing to the high stiffness measured in the odontocete middle ear could be the bony malleal connection to the tympanic. The malleal arm can function either as a cantilever beam or a torsional spring to provide stiffness to the ossicular chain. A restricted or fused arm is typical of high-frequency-hearing species such as microchiropteran bats [1].

C. Comparative Anatomy

Historically, middle-ear acoustic-stiffness measurements in terrestrial mammals were made by measuring acoustic stiffness at the tympanic membrane, whereas our study measured middle-ear point stiffness at the stapes footplate. Two major considerations were necessary to compare our measured results to similar measurements made on terrestrial species. First, to convert from mechanical point stiffness to acoustic stiffness, the point stiffness was divided by the area of the stapes footplate squared. Second, to scale tympanic-membrane measurements to be comparable to acoustic stiffness at the stapes footplate, it was necessary to multiply the stiffness measured at the tympanic membrane by the square of the middle-ear transformer ratio.

Middle-ear transformer ratios have been measured in the cat [19], [20], chinchilla [20], gerbil [21], guinea pig [20], and human [22]. These measurements show a pressure gain averaging 20–30 dB. For species for which measurements of the middle-ear transfer function have not been published, we assumed a middle-ear transfer function of 30. This is justified by the fact that terrestrial middle-ear pressure gains do not appear to be correlated with ear size [23]. By scaling acoustic-stiffness measurements made at the tympanic membrane by the middle-ear transfer function, we can compare measurements of terrestrial species with measurements we made in the bottlenose dolphin.

Fig. 8 shows a comparison of the low-frequency cutoff of 11 different species plotted as a function of the middle-ear stiffness. The low-frequency cutoff was defined to be the frequency with
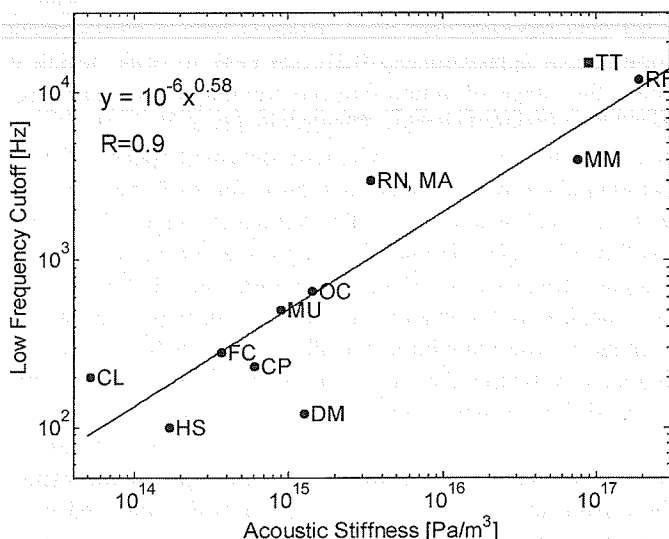

Fig. 8. Relationship between low-frequency cutoff and middle-ear stiffness of various mammalian species. Low-frequency cutoff was determined by selecting the −20 dB point on the behavioral audiogram for each species. Middle-ear stiffness is the equivalent stiffness at the stapes footplate from within the cochlea. The *Tursiops* data point was calculated by dividing the measured point stiffness 1.37 N/μm by the area of stapes footplate squared. The solid line shows power fit to data points. FC: *Felus catus*, cat; audiogram [24], stiffness [25]. CL: *Chinchilla laniger*, chinchilla; audiogram [26], stiffness [27]. CP: *Cavia procellus*, guinea pig; audiogram [28], stiffness [29]. MU: *Meriones unguiculatus*, Mongolian gerbil; audiogram [30], stiffness [31]. MA: *Mesocricetus auratus*, hamster; audiogram [32], stiffness [33]. HS: *Homo sapiens*, human; audiogram [4], stiffness [22]. DM: *Dipodomys merriami*, kangaroo rat; audiogram [34], stiffness [35]. MM: *Mus musculus*, mouse; audiogram [36], stiffness [37]. OC: *Oryctalagus cuniculus*, rabbit; audiogram [36], stiffness [38]. RN: *Rattus norvegicus*, rat; audiogram [39], stiffness [40]. RF: *Rhinolophus ferrumquinum*, horseshoe bat; audiogram [5], stiffness [41], TT: *Tursiops truncatus*, bottlenose dolphin; audiogram [3], stapes area [15].

a threshold 20 dB higher than the frequency of best hearing, and was taken from published audiograms of each species. The solid line in the Fig. 8 shows a power fit through all points shown.

This regression line demonstrates the correlation between middle-ear stiffness and low-frequency cutoff for terrestrial mammals. The proximity of the *Tursiops truncatus* data point suggests that this correlation applies to the bottlenose dolphin as well. If Tursiops ears are representative of most odontocetes, measuring middle-ear stiffness in other odontocete species will allow a prediction of their low-frequency cutoff.

V. CONCLUSION

A novel approach to measuring middle-ear stiffness was used to investigate the point stiffness of the middle ear of the bottlenose dolphin *Tursiops truncatus*. The point stiffness of the middle ear was measured to be 1.37 N/μm, which corresponds to an acoustic stiffness of 1.04×10^{17} Pa/m^3. Therefore, the bottlenose dolphin middle ear is exceptionally stiff compared to most mammalian species and is comparable to that of the horseshoe bat. Correlation between low-frequency hearing cutoff and middle-ear stiffness was demonstrated for terrestrial mammals and is shown to be consistent also for *Tursiops*.

Middle-ear stiffness is an important parameter in the acoustic-power-flow model of the auditory system. Future measurements of the cochlear input impedance Z_C for *Tursiops* will allow the computation of the entire middle-ear transfer function, which

can then be used to predict the low- and middle-frequency portions of the audiogram [13]. This approach may also allow the prediction of hearing capabilities of species that are not available for behavioral testing.

REFERENCES

[1] D. R. Ketten, "Cetacean ears," in *Hearing by Whales and Dolphins*, W. Au, A. S. Popper, and R. Fay, Eds. New York: Springer-Verlag, 2000.

[2] W. W. L. Au, *The Sonar of Dolphins*. New York: Springer-Verlag, 1993.

[3] D. K. Ljungblad, P. D. Scoggins, and W. G. Gilmartin, "Auditory thresholds of a captive Eastern Pacific bottle-nosed dolphin, Tursiops spp," *J. Acoust. Soc. Amer.*, vol. 72, no. 6, pp. 1726–1729, Dec. 1982.

[4] L. L. Jackson, R. S. Heffner, and H. E. Heffner, "Free-field audiogram of the Japanese macaque (Macaca fuscata)," *J. Acoust. Soc. Amer.*, vol. 106, no. 5, pp. 3017–3023, Nov. 1999.

[5] G. R. Long and H. U. Schnitzler, "Behavioral audiograms from the bat, Rhinolophus ferrumequinum," *J. Comp. Physiol.*, vol. 100, no. 3, pp. 211–219, Jan. 1975.

[6] J. J. Rosowski, "Outer and middle ears," in *Comparative Hearing: Mammals*, R. R. Fay and A. N. Popper, Eds. New York: Springer-Verlag, 1994.

[7] G. Fleischer, *Evolutionary Principles of the Mammalian Middle Ear*. New York: Springer-Verlag, 1978.

[8] ——, "On structure and function of the middle ear in the bottlenosed dolphin (Tursiops truncatus)," in *Conf. Biological Sonar and Diving Mammals*, Menlo Park, CA, 1972.

[9] J. G. McCormick, E. G. Wever, S. H. Ridgeway, and J. Palin, "Sound reception in the porpoise as it relates to echolocation," in *Animal Sonar Systems*, R. G. Busnel and J. F. Fish, Eds. New York: Plenum, 1980, p. xxiv.

[10] E. G. Wever, J. G. McCormick, J. Palin, and S. H. Ridgway, "Cochlea of the dolphin, Tursiops truncatus: The basilar membrane," *Proc. Nat. Acad. Sci. U.S.A.*, vol. 68, no. 11, pp. 2708–2711, Nov. 1971.

[11] K. S. Norris, "Peripheral sound processing in odontocetes," in *Animal Sonar Systems*, R. G. Busnel and J. F. Fish, Eds. New York: Plenum, 1980, p. xxiv.

[12] M. A. Ruggero and A. N. Temchin, "The roles of the external, middle, and inner ears in determining the bandwidth of hearing," *Proc. Nat. Acad. Sci. U.S.A.*, vol. 99, no. 20, pp. 13 206–13 210, Oct. 2002.

[13] D. C. Mountain, A. E. Hubbard, D. R. Ketten, and J. T. O'Malley, "The helicotrema: Measurements and models," in *Int. Symp. Biophysics Cochlea: From Molecules to Models*, Titisee, Germany, 2002.

[14] S. Hemila, S. Nummela, and T. Reuter, "A model of the odontocete middle ear," *Hear. Res.*, vol. 133, no. 1–2, pp. 82–97, Jul. 1999.

[15] S. Nummela, T. Wagar, S. Hemila, and T. Reuter, "Scaling of the cetacean middle ear," *Hear. Res.*, vol. 133, no. 1–2, pp. 71–81, Jul. 1999.

[16] E. S. Olson and D. C. Mountain, "In vivo measurement of basilar membrane stiffness," *J. Acoust. Soc. Amer.*, vol. 89, no. 3, pp. 1262–1275, Mar. 1991.

[17] G. Emadi, C. P. Richter, and P. Dallos, "Stiffness of the gerbil basilar membrane: Radial and longitudinal variations," *J. Neurophysiol.*, vol. 91, no. 1, pp. 474–488, Jan. 2004.

[18] M. E. Ravicz, S. N. Merchant, and J. J. Rosowski, "Effect of freezing and thawing on stapes-cochlear input impedance in human temporal bones," *Hear. Res.*, vol. 150, no. 1–2, pp. 215–224, Dec. 2000.

[19] L. Decory, R. B. Franke, and A. L. Dancer, "Measurement of the middle ear transfer function in cat, chinchilla, and guinea pig," in *The Mechanics and Biophysics of Hearing*, P. Dallos, C. D. Geisler, J. W. Matthews, M. A. Ruggero, and C. R. Steele, Eds. Berlin, Germany: Springer-Verlag, 1990, pp. 270–277.

[20] V. Nedzelnitsky, "Sound pressures in the basal turn of the cat cochlea," *J. Acoust. Soc. Amer.*, vol. 68, no. 6, pp. 1676–1689, Dec. 1980.

[21] E. S. Olson, "Observing middle and inner ear mechanics with novel intracochlear pressure sensors," *J. Acoust. Soc. Amer.*, vol. 103, no. 6, pp. 3445–3463, Jun. 1998.

[22] S. Puria, W. T. Peake, and J. J. Rosowski, "Sound-pressure measurements in the cochlear vestibule of human-cadaver ears," *J. Acoust. Soc. Amer.*, vol. 101, no. 5, pp. 2754–2770, May 1997.

[23] S. Hemila, S. Nummela, and T. Reuter, "What middle ear parameters tell about impedance matching and high frequency hearing," *Hear. Res.*, vol. 85, no. 1–2, pp. 31–44, May 1995.

[24] R. S. Heffner and H. E. Heffner, "Hearing range of the domestic cat," *Hear. Res.*, vol. 19, no. 1, pp. 85–88, 1985.

[25] J. J. Guinan Jr. and W. T. Peake, "Middle-ear characteristics of anesthetized cats," *J. Acoust. Soc. Amer.*, vol. 41, no. 5, pp. 1237–1261, May 1967.

[26] R. S. Heffner and H. E. Heffner, "Behavioral hearing range of the chinchilla," *Hear. Res.*, vol. 52, no. 1, pp. 13–16, Mar. 1991.

[27] P. A. Vrettakos, S. P. Dear, and J. C. Saunders, "Middle ear structure in the chinchilla: A quantitative study," *Amer. J. Otolaryngol.*, vol. 9, no. 2, pp. 58–67, Mar./Apr. 1988.

[28] R. Heffner, H. Heffner, and B. Masterton, "Behavioral measurements of absolute and frequency-difference thresholds in guinea pig," *J. Acoust. Soc. Amer.*, vol. 49, no. 6, pp. 1888–1895, Jun. 1971.

[29] M. E. Ravicz, "Acoustic impedance of the gerbil ear," M.S. thesis, Boston University, Boston, MA, 1990.

[30] A. Ryan, "Hearing sensitivity of the Mongolian gerbil, Meriones unguiculatis," *J. Acoust. Soc. Amer.*, vol. 59, no. 5, pp. 1222–1226, May 1976.

[31] M. E. Ravicz, J. J. Rosowski, and H. F. Voigt, "Sound-power collection by the auditory periphery of the Mongolian gerbil Meriones unguiculatus. I: Middle-ear input impedance," *J. Acoust. Soc. Amer.*, vol. 92, no. 1, pp. 157–177, Jul. 1992.

[32] R. S. Heffner, G. Koay, and H. E. Heffner, "Audiograms of five species of rodents: Implications for the evolution of hearing and the perception of pitch," *Hear. Res.*, vol. 157, no. 1–2, pp. 138–152, Jul. 2001.

[33] D. Zwillenberg, D. F. Konkle, and J. C. Saunders, "Measures of middle ear admittance during experimentally induced changes in middle ear volume in the hamster," *Otolaryngol. Head Neck Surg.*, vol. 89, no. 5, pp. 856–860, Sep./Oct. 1981.

[34] P. Dallos, "Low-frequency auditory characteristics: Species dependence," *J. Acoust. Soc. Amer.*, vol. 48, no. 2, pp. 489–499, Aug. 1970.

[35] D. B. Webster and M. Webster, "Auditory systems of heteromyidae: Cochlear diversity," *J. Morphol.*, vol. 152, no. 2, pp. 153–169, May 1977.

[36] H. Heffner and B. Masterton, "Hearing in glires domestic rabbit cotton rat feral house mouse and kangaroo rat," *J. Acoust. Soc. Amer.*, vol. 68, no. 6, pp. 1584–1599, Dec. 1980.

[37] J. C. Saunders and R. M. Summers, "Auditory structure and function in the mouse middle ear: An evaluation by SEM and capacitive probe," *J. Comp. Physiol., A*, vol. 146, no. 4, pp. 517–525, Dec. 1982.

[38] A. R. Moller, "An experimental study of the acoustic impedance of the middle ear and its transmission properties," *Acta Otolaryngol.*, vol. 60, pp. 129–149, Jul./Aug. 1965.

[39] H. E. Heffner, R. S. Heffner, C. Contos, and T. Ott, "Audiogram of the hooded Norway rat," *Hear. Res.*, vol. 73, no. 2, pp. 244–247, Mar. 1994.

[40] R. Mundie, "The Impedance of the Ear—A Variable Quantity ," *Middle Ear Function Seminar*, pp. 63–85, 1963. U. S. Army Medical Research Laboratory Rep. No. 576.

[41] J. P. Wilson and V. Bruns, "Middle-ear mechanics in the CF-bat Rhinolophus ferrumequinum," *Hear. Res.*, vol. 10, no. 1, pp. 1–13, Apr. 1983.

Brian S. Miller received the B.Sc. degree in biology and biomedical engineering from Boston University, Boston, MA, in 2003. He is currently pursuing a graduate degree in marine science at the University of Otago, New Zealand.

From 2003 to 2005, he was a Research Assistant at the Boston University Hearing Research Center.

Aleks L. Zosuls grew up on Long Island, NY. He received the B.Sc. degree in biomedical engineering from Boston University, Boston, MA, in 2001.

Since then, he has been working as a Research Assistant at Boston University in the Hearing Research Center and the VLSI laboratory. His research includes cochlear mechanics, biomimetic signal processing hardware, Cetacean hearing research, and VLSI chip testing.

Darlene R. Ketten received the B.A. degree in biology and french from Washington University, Seattle, in 1971, the M.S. degree in biological oceanography from Massachusetts Institute of Technology, Cambridge, in 1979, and the Ph.D. degree from the Johns Hopkins University, Baltimore, MD, (jointly awarded neuroanatomy, behavioral ecology, and experimental radiology), in 1984.

She is a Marine Biologist and a Neuroanatomist specializing in functional and biomedical imaging of sensory systems. She currently holds joint appointments as a Senior Scientist in Biology at Woods Hole Oceanographic Institution, Woods Hole, MA, and as an Assistant Professor in Otology and Laryngology at Harvard Medical School, Boston, MA. Her speciality training includes otopathology at Harvard Medical School, in 1987, neuroradiology at Armed Forces Institute of Pathology (AFIP), in 2003, veterinary pathology at AFIP, in 2005, and forensic pathology at AFIP, in 1995 and 2005. She serves as a Specialty Lecturer on inner ear imaging, anatomy, and diagnostic pathology for American Medical Association—head and neck surgery courses. Her research focuses on two areas: how structural differences in marine versus terrestrial-vertebrate ears relate to physical differences habitats and feeding behaviors and how electrode placement and inner-ear pathologies impact the effectiveness of cochlear implants.
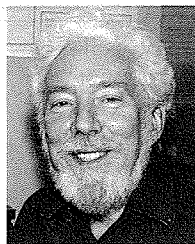
David C. Mountain received the B.Sc. degree in electrical engineering from the Massachusetts Institute of Technology (MIT), Cambridge, in 1968, the M.S. degree in electrical engineering and the Ph.D. degree, both from the University of Wisconsin, Madison, in 1973 and 1978, respectively.

He was a member of the Medical Engineering Department at Massachusetts General Hospital, Boston, from 1968 to 1970. He joined the Boston University faculty in 1979, where he is now Professor of Biomedical Engineering. His current research emphasis is on experimental and theoretical studies in auditory biomechanics, neuroinformatics, and biomimetic acoustic signal processing.

Dr. Mountain is a fellow of the American Institute for Medical and Biological Engineering.